Understanding Quantum Tunneling through Quantum Monte Carlo Simulations

Sergei V. Isakov, Guglielmo Mazzola, Vadim N. Smelyanskiy, Zhang Jiang, Sergio Boixo, Hartmut Neven, and Matthias Troyer

Phys. Rev. Lett. **117**, 180402 — Published 28 October 2016

DOI: 10.1103/PhysRevLett.117.180402

Understanding Quantum Tunneling through Quantum Monte Carlo Simulations

Sergei V. Isakov,[1] Guglielmo Mazzola,[2] Vadim N. Smelyanskiy,[3]
Zhang Jiang,[4,5] Sergio Boixo,[3] Hartmut Neven,[3] and Matthias Troyer[2]

[1] *Google, 8002 Zurich, Switzerland*
[2] *Theoretische Physik, ETH Zurich, 8093 Zurich, Switzerland*
[3] *Google, Venice, CA 90291, USA*
[4] *QuAIL, NASA Ames Research Center, Moffett Field, CA 94035, USA*
[5] *Stinger Ghaffarian Technologies Inc., 7701 Greenbelt Rd., Suite 400, Greenbelt, MD 20770, USA*

The tunneling between the two ground states of an Ising ferromagnet is a typical example of many-body tunneling processes between two local minima, as they occur during quantum annealing. Performing quantum Monte Carlo (QMC) simulations we find that the QMC tunneling rate displays the same scaling with system size, as the rate of incoherent tunneling. The scaling in both cases is $O(\Delta^2)$, where Δ is the tunneling splitting (or equivalently the minimum spectral gap). An important consequence is that QMC simulations can be used to predict the performance of a quantum annealer for tunneling through a barrier. Furthermore, by using open instead of periodic boundary conditions in imaginary time, equivalent to a projector QMC algorithm, we obtain a quadratic speedup for QMC, and achieve linear scaling in Δ. We provide a physical understanding of these results and their range of applicability based on an instanton picture.

Quantum annealing [1–6] (QA) has been proposed as a method to solve combinatorial optimization problems. In contrast to its closely related classical counterpart, simulated annealing (SA) [7], which makes use of thermal fluctuations to escape local minima of the energy landscape in the search for a low energy solution, QA can additionally exploit quantum tunneling. In QA the system closely follows the ground state of a time-dependent Hamiltonian $H(t)$ whose initial ground state at $t = 0$ is easy to prepare. The final Hamiltonian $H(t_{\rm final})$ encodes the cost function of a combinatorial optimization problem.

Random ensembles of hard problems are closely connected to spin glass models known in statistical physics. There one typically passes through a second order quantum phase transition from a paramagnetic into a glassy phase, where the energy gap closes polynomially with problem size N, and then encounters a cascade of avoided level crossings with typically exponentially small gaps $\Delta \propto e^{-\alpha N}$ inside the glassy phase [3, 8–10]. In other problems, such as Grover search or number partitioning, there may just be a single exponentially small gap at a single first order quantum phase transition. Avoided level crossings with exponential gaps are the main bottleneck in quantum annealing and are in most cases associated with tunneling processes.

Simulations are important to understand the mechanisms of QA and find the class of problems for which QA may perform better than SA and other classical algorithms. QMC simulations have been performed [3, 11, 12] on problems of much larger sizes than accessible by direct integration of the time dependent Schrödinger equation. In particular, a recent numerical study of random Ising spin glass instances [12] has reconciled expectations of quantum speedup based on QMC simulations [3] with experiments that failed to detect it [5].

The major bottlenecks of QMC simulations of QA are also associated with tunneling events. However, while QMC faithfully samples the equilibrium thermal state of a quantum system it does not directly simulate its unitary time evolution. In particular, the universal critical exponents at second order quantum phase transitions are different than those of the stochastic QMC dynamics, as was recently pointed out in this context [13]. Nevertheless, correlations between QMC dynamics and the gap have recently been observed in simple models [14].

In this Letter we show that despite the different dynamics there exists a broad class of tunneling problems where QMC is not "merely" a quantum-inspired classical optimization algorithm [3–5]. In these problems the time of QMC to simulate quantum mechanical tunneling scales identically (in leading exponential order) with the problem size to the tunneling rate of a physical system and QMC is thus a quantitatively faithful predictor of QA performance. We also discuss possible types of problems where this may not apply.

Tunneling in a transverse field Ising model — To establish the equivalence of QA and QMC tunneling dynamics in the case of quantum spin systems we study the archetypical model of an Ising ferromagnet in the presence of a weak transverse field Γ with Hamiltonian $H = -\Gamma \sum \sigma_j^x - \sum J_{ij}\sigma_i^z\sigma_j^z$, considering both a linear chain with couplings $J_{ij} = (\delta_{i,j+1} + \delta_{i,j-1})/2$ and fully connected clusters with $J_{ij} = 1/2L$, where L is the number of spins.

For small Γ there are two degenerate ground states: the configuration labeled $|\uparrow\rangle$ with spins aligned pointing (predominantly) up and average magnetization per site $m \equiv \frac{1}{L}\sum_i \langle\sigma_i^z\rangle \approx +1$ and the configuration labeled $|\downarrow\rangle$ with $m \approx -1$. For finite L the transverse field term mixes the two states with an exponentially small (in L) but nonzero tunneling matrix element $\epsilon = \langle\uparrow|H|\downarrow\rangle$. This lifts

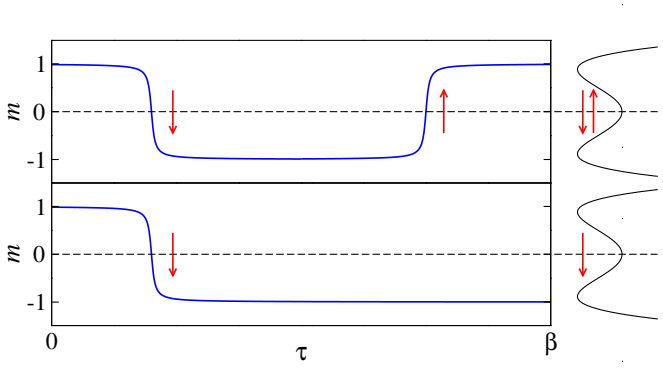

Figure 1. *Upper panel:* Typical instanton/anti-instanton trajectory with periodic boundary condition in imaginary time. Along such trajectories the path samples both the $|\uparrow\rangle$ and $|\downarrow\rangle$ states. The magnetization m exhibits two jumps corresponding to instantons (tunneling events) in imaginary time (red arrows). *Lower panel:* with open boundary condition only one instanton is required and the tunneling probability thus increased. On the right we sketch the double-well potential.

the degeneracy between the two ground states, resulting in an exponentially small energy gap $\Delta = 2\epsilon$ between the states $|\psi_\pm\rangle = 1/\sqrt{2}\,(|\uparrow\rangle \pm |\downarrow\rangle)$. This expression for the gap is also valid in a general case of avoided level crossings when the system can be approximated by a two-level system.

Adiabatically tuning a (weak) longitudinal field $-h\sum_i \sigma_i^z$ from a small positive to a small negative value, we encounter a tunneling problem, which is similar to the typical tunneling problem of QA at avoided level crossings, with the spins having to tunnel from $|\uparrow\rangle$ to $|\downarrow\rangle$.

Tunneling in path integral QMC — QMC simulations are performed by sampling imaginary time paths, obtained from a mapping of the partition function of a D-dimensional quantum system to a $(D+1)$-dimensional classical path integral configuration, which consist of P replicas of the same physical system with spins $S_{i,\tau} = \pm 1$ where the index $i = 1, \cdots, L$ denotes the spatial index and the index $\tau = 1, \cdots, P$ labels the time slices. Our QMC simulations have been performed both with a large number of replicas $P = 128$ in order to be close to the physical continuous time limit, and also directly in the continuous time limit [15]. For updates we use variants of the Wolff [16] and Swendsen-Wang algorithm [17] to build local (in space) clusters along the imaginary time direction [18].

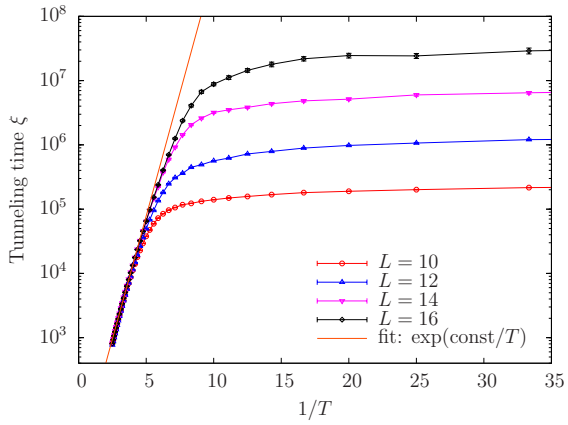

Figure 2. Path integral QMC transition time ξ as a function of the inverse temperature for a chain at $\Gamma = 0.7$. At high temperatures ξ is independent of the system size L and suppressed as $\exp(-E_{\rm barrier}/T)$. At low temperatures, quantum tunneling becomes more efficient and depends only on L.

During the QMC simulation the total magnetization $m(\tau) \equiv \frac{1}{L}\sum_{i=1}^{L} S_{i,\tau}$ evolves stochastically in Monte Carlo time t. Preparing the system in the vicinity of a local minimum, for example by choosing $S_{i,\tau} = 1$, most of the time all replicas sample spin configurations which are fluctuations around the same minimum energy configuration, i.e. $m(\tau) \approx 1$. Every now and then the path $m(\tau, t)$ evolves towards a transition state $m^{**}(\tau)$ corresponding to the saddle point of the free energy functional $\mathcal{F}[m(\tau)]$ of the classical spin model. This saddle point corresponds to an instanton/anti-instanton pair [19] (see Fig. 1 and Ref. [20]). The instantonic path $m^{**}(\tau)$ costs energy as it creates two domain walls in the imaginary time axis, which separate replicas which opposite magnetization $m(\tau)$. These domain walls can diffuse in opposite directions around the imaginary time loop, changing the total manetization to $m(\tau) = -1\ \forall\,\tau$ when they annihilate, signaling the completion of a tunneling event. The creation of $m^{**}(\tau)$ represents the rate-limiting process of tunneling decay in both QMC and QA whose rate is $\propto \Delta^2$ (see below).

To measure the tunneling time ξ we start QMC simulations in a fully polarized state with $m(\tau) = 1$ and measure the number of QMC sweeps (defined as one attempted update per spin) required to obtain a well separated instanton/anti-instanton pair. We detect the latter by requiring that at least the 25% of the replicas reverse their magnetization to $m(\tau) = -1$ [21].

We note that coupling to an environment could lead to thermally activated events, whose pathways traverses the high energy states $m \approx 0$ with energy $E_{\rm barrier} \sim L/2$ for a fully connected cluster and $E_{\rm barrier} \sim 4$ for a linear chain. These are suppressed by a factor $\exp(-\beta E_{\rm barrier})$ and at low temperatures quantum tunneling becomes advantageous, as shown in Fig. 2.

In Fig. 3 we show the measured average tunnelling time ξ in QMC fully connected clusters as a function of L and Γ and observe an exponential scaling with L. The data are well fitted by $aL^{-1}\exp(bL)$ (see Ref. [20] for analytical derivation in a semiclassical approach). There is only a very weak temperature dependence for QMC in the low temperature quantum regime, mostly due to instanton diffusion. As shown in Fig. 3 the scaling of QMC simulations is identical to $1/\Delta^2$ within error bars, thus

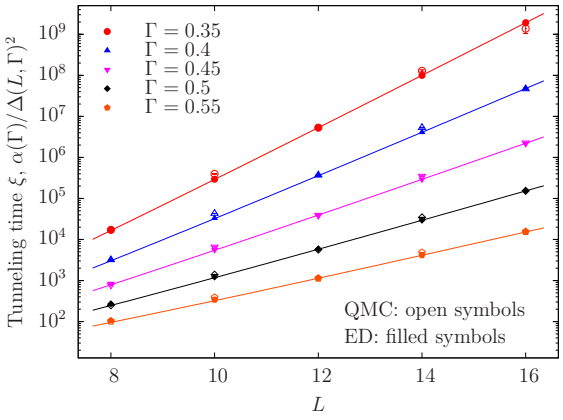

Figure 3. Average QMC tunneling time ξ as a function of system size L (open symbols) for a fully connected graph at $\beta = 8$ for various values of the transverse field Γ. Fits of the times for $8 \le L \le 16$ are shown as solid lines. To compare to physical QA we also show $\alpha(\Gamma)/\Delta(\Gamma, L)^2$ with filled symbols, obtained by exact diagonalization. Rescaling by L-independent constants $\alpha(\Gamma)$ we find identical scaling with system size L.

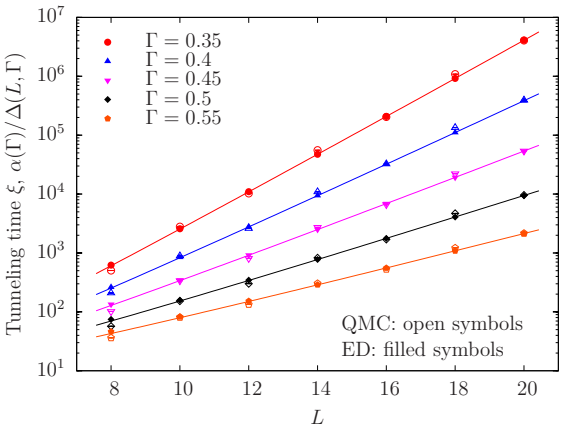

Figure 4. (color online). Average PIGS tunneling time ξ as a function of L (open symbols) for a fully connected graph at $\beta = 8$ with various values of the transverse field Γ. Fits of the times for $8 \le L \le 20$ are shown as solid lines. Points proportional to $1/\Delta(L)$, obtained with exact diagonalization, are shown with filled symbols.

confirming the identical scaling behavior of both types of dynamics. The same behavior is observed for linear chains [20]. We validate these findings by simulations of tunneling in a one-dimensional double well potential $V(x) = \lambda x^4 - x^2$, where Δ depends exponentially on λ. Performing QMC simulations in continuous space [22] we compared the average QMC tunneling time to $1/\Delta^2$ and find excellent agreement over a wide range of time scales [20]. Furthermore, we find that the QMC scaling does not significantly depend on whether local or global updates are used.

Accelerating tunneling in QMC — We expect a quadratic speedup for QMC with open (OBC) instead of periodic boundary conditions (PBC) in imaginary time as in this case only one domain wall (instanton) is created in the magnetization reversing process (see Fig. 1). Indeed, as shown in Fig. 4 and Table I of Ref. [20] the scaling exponent is reduced by a factor of two compared to QMC with PBC and open system QA, and the tunneling time now scales as $1/\Delta$ instead of $1/\Delta^2$. The data are well fitted by $aL^{-1/2}\exp(bL)$. Using OBC describes a so-called path integral ground state (PIGS) simulation [23]. PIGS algorithm can be viewed as projecting from a trial state (given by the boundary conditions in imaginary time) and sampling from the ground state wave function at large enough β, hence providing the tunneling probability amplitude that is proportional to Δ. This finding may explain the recently observed superiority of QMC projecting techniques compared to PIMC in continuous space models [24].

Tunneling decay of a metastable state — To gain insight into the equivalence of QA and QMC we consider the tunneling between two nearly degenerate minima $\mathbf{x}_1$ and $\mathbf{x}_2$ of a potential $V(\mathbf{x})$ with continuous variable $\mathbf{x}$. The pioneering work of Langer [25, 26] makes an explicit connection between the tunneling rate of a particle and the classical Kramers escape rate from the metastable state of a non-linear stochastic field process. This sheds light on how QA and QMC tunneling dynamics are related.

Within a semiclassical picture, the wave function decays exponentially in the classically forbidden region. In the particular case where the action under the barrier is purely imaginary this corresponds to a particle moving with imaginary momentum along the imaginary time axis $t = -i\tau$ [27, 28]. The amplitude of tunneling from the ground state associated with a local minimum $V(\mathbf{x}_1) = 0$ is determined by the path integral $K_\tau(\mathbf{x}', \mathbf{x}_1) = \int D[\mathbf{x}(\tau')]\ e^{-\mathcal{S}_\tau[\mathbf{x}(\tau')]/\hbar}$ between the local minimum $\mathbf{x}(0) \approx \mathbf{x}_1$ and the turning point $\mathbf{x}(\tau) = \mathbf{x}'$ at the barrier exit chosen to maximize K_τ. Here $\mathcal{S}_\tau[\mathbf{x}(\tau')] = \int_0^\tau d\tau' \frac{1}{2} m\dot{\mathbf{x}}^2(\tau') + V(\mathbf{x}(\tau'))$ is the action of the path under the barrier and $\tau \to \infty$. The dominant contribution comes from the stationary action path (instanton) $\mathbf{x}^*(\tau')$ corresponding to a particle moving in the inverted potential $-V(\mathbf{x})$. The tunneling amplitude is proportional to $\exp(-\mathcal{S}_\tau[\mathbf{x}^*(\tau')]/\hbar)$.

Similar arguments are known in statistical physics where the partition function $\mathcal{Z} = \mathrm{Tr}\, K_\beta$ of a state thermalized near a local minimum $\mathbf{x}_1$ of the potential corresponds to the path integral in imaginary time with PBC for $\mathbf{x}(\tau)$ with $0 \le \tau < \beta = \hbar/k_B T$. By tunneling away from the minimum, the partition function acquires an imaginary part. It is dominated by the instanton/anti-instanton path $\mathbf{x}^{**}(\tau)$ that moves under the barrier starting near $\mathbf{x}_1$, reaches the turning point $\mathbf{x}'$, and returns [19]. We note that $-2\,\mathrm{Im}\mathcal{Z}/(\beta\,\mathrm{Re}\mathcal{Z}) \propto \Delta^2$ [29] gives a *squared* tunneling amplitude ($\propto e^{-\mathcal{S}_\beta[x^{**}(\tau)]/\hbar}$) because we pay the cost of creating an instanton and an anti-

instanton.

In the context of QA we introduce a slowly varying field that changes the order of the minima $\mathbf{x}_{1,2}$ of $V(\mathbf{x},t)$. At the start of QA the system is localized in the vicinity of $\mathbf{x}_1$ and at the end it arrives at the vicinity of $\mathbf{x}_2$ after a tunneling event at time t_c when $V(\mathbf{x}_1,t_c) \approx V(\mathbf{x}_2,t_c)$. In the case of open system QA when the dephasing time $T_2 \ll \Delta^{-1}$ there is incoherent tunneling at $t \approx t_c$ from $\mathbf{x}_1$ to $\mathbf{x}_2$ with rate $T_2\,\Delta^2$, determining the time scale of open system QA [30–32]. The same scaling with Δ^2 is also obtained in closed systems by the Landau-Zener formula.

Following Refs. [25, 26], the tunneling decay rate *formally* corresponds to the Kramers escape rate from a metastable state of a classical 1D field with order parameter $\mathbf{x}(\tau)$ satisfying the PBC and free energy functional $\mathcal{F} = \mathcal{S}_\beta[\mathbf{x}(\tau)]/\beta$. The stochastic evolution of this field $\mathbf{x}(\tau,t)$ in time t is described by the Langevin equation $\mathbf{x}_t = -\mu\beta^{-1}[\boldsymbol{\nabla} V - m\mathbf{x}_{\tau\tau}] + (2\mu\hbar/\beta)^{1/2}\,\boldsymbol{\eta}$, where $\boldsymbol{\eta}(\tau,t)$ is a random force delta correlated in both of its arguments and μ is a relaxation coefficient. We now observe that the same dynamics describes the standard path integral QMC to calculate the partition function $\mathcal{Z}$. QMC samples paths $\mathbf{x}(\tau,t)$ with sweeping rate $\propto \mu$. The functional $\mathcal{F}[\mathbf{x}(\tau)]$ has a saddle point $\mathbf{x}^{**}(\tau)$ that the QMC trajectory $\mathbf{x}(\tau,t)$ crosses during the escape event from the metastable state $\mathbf{x}_1$ towards $\mathbf{x}_2$. According to Kramers theory the escape rate is $W \propto e^{-\mathcal{F}/k_BT} = e^{-\mathcal{S}_\beta[\mathbf{x}^{**}(\tau)]/\hbar}$. This saddle point is precisely the instanton/anti-instanton path, and therefore the QMC escape rate $W \propto \Delta^2 \propto -\mathrm{Im}\,\mathcal{Z}$. Therefore, in this archetypical example, the time needed for a physical system to tunnel has the same exponential factor as the corresponding simulation time of quantum Monte Carlo. In the case of OBC in imaginary time, the tunneling trajectory is dominated by configurations with a single instanton $\mathbf{x}^*(\tau)$ with corresponding escape rate $W \propto \Delta$ – giving quadratic speedup of QMC over incoherent tunneling.

The semiclassical instanton picture is applicable to tunneling in the fully-connected mean-field models of quantum spins with p-body interactions and a transverse field and in other models, in which tunneling transitions occur via simultaneous collective reorganization of large groups of spins. The above numerical study considers one such model. The semiclassical approach becomes asymptotically exact in the limit of large number of spins $L \gg 1$ and it has been recently applied to this model class (see, e.g., [33, 34] and also Sec. II of Ref. [20]). The coordinate of the instanton trajectory in this case corresponds to the total magnetization $m(\tau)$ per spin. It t is possible to establish a direct correspondence between the quantum instanton and saddle point of the free energy functional corresponding to the Gibbs probability measure in QMC updates (see Sec. III in Ref. [20]). This provides a theoretical basis using Kramers escape theory for the above numerical results connecting the scaling exponents for tunneling rates to the corresponding scaling of the QMC.

Potential obstructions for QMC — While our findings apply to tunneling in a broad class of mean field models with purely imaginary time instantons, we shall also mention several areas where obstructions for the efficient simulation of quantum tunneling with QMC might exist.

QMC sampling may sometimes be inefficient due to topological obstructions such as winding numbers of world lines [35]. While PIGS simulations often solve this problem by cutting the PBC, an obstruction remains if the ground state wave function and its square are concentrated on different supports [35] – although suitable trial wave functions at the boundaries of the path integral can alleviate this problem. Conversely, the quantum system might have conserved quantum numbers that limit tunneling paths to a lower-dimensional subspace than that explored by QMC [20].

QMC may also be less efficient in optimization problems that require tunneling to or from multidimensional minima. In such problems the semiclassical action under the barrier $S(\mathbf{x})$ is often not purely imaginary and displays complex features due to the presence of caustics, non-integrability and non-analyticity [28, 36]. Due to a highly oscillating nature of the wave function in the classically forbidden region it is not clear if the tunneling dynamics can be faithfully recovered with QMC.

Another important open question arises in problems that exhibit a many-body location/delocalization transition at finite values of transverse field [37]. There a delocalized phase can exist in a range of energies with exponentially many local minima separated by large Hamming distances and connected by a large number of tunneling paths [38]. QA, in contrast to QMC dynamics, may profit from the positive interference between exponentially many paths.

We also note that the polynomial prefactors can be different for QMC and QA even in the cases when tunneling is described by mean field models with purely imaginary time instantons.

Conclusions — We conclude by discussing the consequences of our results for quantum annealing. Despite QMC dynamics being different from unitary evolution, the relevance of instanton configurations for tunneling processes in a class of models with purely imaginary time instantons leads to the same exponential scaling of tunneling rate through a tall barrier in both cases. A consequence of this equivalence is that QMC simulations are predictive of the performance of QA for hard optimization problems where the performance is limited by such tunneling events.

We also observed that is some cases a version of QMC with OBC (PIGS) can provide a quadratic speedup. While one can, theoretically, recover such a quadratic speedup [39] in QA if the evolution of the energy gap is exactly known and if the tunneling is fully coherent [31],

this protocol can hardly be realized in practical QA. Nevertheless, a quadratic speed up can be achieved with polynomial overhead on a universal quantum computer using an approach that relaxes the above conditions [40].

These findings demonstrate that QMC simulations can be used as a powerful and predictive tool to investigate optimization problems amenable to quantum annealing. Our study demonstrates that the quest for quantum speedup using a physical quantum annealer must focus on the problems and hardware that allows to reach *beyond* the class of problems discussed in this paper where the identical scaling of QMC and QA preclude a scaling advantage and where PIGS can achieve a quadratic speedup for tunneling through individual barriers. The absence of calibration and programming errors, the flexibility in simulating arbitrary graph topologies without the need to embed into a hardware graph, and the observed quadratic speedup for tunneling through individual barriers in PIGS simulations makes QMC a competitive classical technology. Nevertheless, a physical QA can still be many orders of magnitude faster than QMC simulations [41]. We expect that the physical mechanisms behind the possible obstructions for QMC discussed above will provide interesting starting points for future studies of potential quantum speedup. In particular, one has to explore the power of QA with non-stoquastic Hamiltonians for which the negative sign problem prevents a matching QMC algorithm.

The work of GM and MT has been supported by the Swiss National Science Foundation through the National Competence Center in Research QSIT and by ODNI, IARPA via MIT Lincoln Laboratory Air Force Contract No. FA8721-05-C-0002. MT acknowledges hospitality of the Aspen Center for Physics, supported by NSF grant #PHY–1066293. We acknowledge useful discussions with F. Becca, M. Dykman, and G. Santoro.

[1] T. Kadowaki and H. Nishimori, Phys. Rev. E **58**, 5355 (1998).
[2] E. Farhi, J. Goldstone, S. Gutmann, J. Lapan, A. Lundgren, and D. Preda, Science **292**, 472 (2001).
[3] G. E. Santoro, R. Martonak, E. Tosatti, and R. Car, Science **295**, 2427 (2002).
[4] S. Boixo, T. F. Ronnow, S. V. Isakov, Z. Wang, D. Wecker, D. A. Lidar, J. M. Martinis, and M. Troyer, Nature Physics **10**, 218 (2014).
[5] T. F. Rønnow, Z. Wang, J. Job, S. Boixo, S. V. Isakov, D. Wecker, J. M. Martinis, D. A. Lidar, and M. Troyer, Science **345**, 420 (2014).
[6] J. King, S. Yarkoni, M. M. Nevisi, J. P. Hilton, and C. C. McGeoch, arXiv:1508.05087.
[7] S. Kirkpatrick, C. D. Gelatt, and M. P. Vecchi, Science **220**, 671 (1983).
[8] B. Altshuler, H. Krovi, and J. Roland, Proceedings of the National Academy of Sciences **107**, 12446 (2010).
[9] E. Farhi, D. Gosset, I. Hen, A. W. Sandvik, P. Shor, A. P. Young, and F. Zamponi, Phys. Rev. A **86**, 052334 (2012).
[10] S. Knysh, Nat. Commun. **7**, 12370 (2016).
[11] R. Martoňák, G. E. Santoro, and E. Tosatti, Phys. Rev. B **66**, 094203 (2002).
[12] B. Heim, T. F. Rønnow, S. V. Isakov, and M. Troyer, Science **348**, 215 (2015).
[13] C.-W. Liu, A. Polkovnikov, and A. W. Sandvik, Phys. Rev. Lett. **114**, 147203 (2015).
[14] L. T. Brady and W. van Dam, Phys. Rev. A **93**, 032304 (2016).
[15] H. Rieger and N. Kawashima, Eur. Phys. J. B **9**, 233 (1999).
[16] U. Wolff, Phys. Rev. Lett. **62**, 361 (1989).
[17] R. H. Swendsen and J.-S. Wang, Phys. Rev. Lett. **58**, 86 (1987).
[18] S. V. Isakov and R. Moessner, Phys. Rev. B **68**, 104409 (2003).
[19] A. I. Vainshtein, V. I. Zakharov, V. A. Novikov, and M. A. Shifman, Soviet Physics Uspekhi **25**, 195 (1982).
[20] See Supplemental Material at [url], which includes references [3, 22, 33, 34, 42–50], for additional quantum Monte Carlo results and details of analytical calculations.
[21] The number 25% is somewhat arbitrary but we find that waiting until all, 25% or 2% of the replicas reverse magnetization makes only small differences.
[22] D. M. Ceperley, Rev. Mod. Phys. **67**, 279 (1995).
[23] A. Sarsa, K. E. Schmidt, and W. R. Magro, J. Chem. Phys. **113**, 1366 (2000).
[24] E. M. Inack and S. Pilati, Phys. Rev. E **92**, 053304 (2015).
[25] J. S. Langer, Annals of Physics **41**, 108 (1967).
[26] J. S. Langer, Annals of Physics **54**, 258 (1969).
[27] S. Coleman, Phys. Rev. D **15**, 2929 (1977).
[28] S. Takada and H. Nakamura, J. Chem. Phys. **100**, 98 (1994).
[29] E. M. Chudnovsky and J. Tejada, *Macroscopic Quantum Tunneling of the Magnetic Moment* (Cambridge, UK: Cambridge University Press, 1998).
[30] M. H. S. Amin and D. V. Averin, Phys. Rev. Lett. **100**, 197001 (2008).
[31] M. H. S. Amin, D. V. Averin, and J. A. Nesteroff, Phys. Rev. A **79**, 022107 (2009).
[32] S. Boixo, V. N. Smelyanskiy, A. Shabani, S. V. Isakov, M. Dykman, V. S. Denchev, M. Amin, A. Smirnov, M. Mohseni, and H. Neven, arXiv:1411.4036.
[33] V. Bapst and G. Semerjian, Journal of Statistical Mechanics: Theory and Experiment **2012**, P06007 (2012).
[34] K. Kechedzhi and V. N. Smelyanskiy, Phys. Rev. X **6**, 021028 (2016).
[35] M. B. Hastings, Quantum Information & Computation **13**, 1038 (2013).
[36] Z. H. Huang, T. E. Feuchtwang, P. H. Cutler, and E. Kazes, Phys. Rev. A **41**, 32 (1990).
[37] C. R. Laumann, R. Moessner, A. Scardicchio, and S. L. Sondhi, Eur. Phys. J. Special Topics **224**, 75 (2015).
[38] C. R. Laumann, A. Pal, and A. Scardicchio, Phys. Rev. Lett. **113**, 200405 (2014).
[39] J. Roland and N. J. Cerf, Phys. Rev. A **65**, 042308 (2002).
[40] S. Boixo, E. Knill, and R. D. Somma, arXiv:1005.3034 (2010).
[41] V. S. Denchev, S. Boixo, S. V. Isakov, N. Ding, R. Babbush, V. Smelyanskiy, J. Martinis, and H. Neven, Phys.

Rev. X **6**, 031015 (2016).
[42] M. E. Tuckerman, B. J. Berne, G. J. Martyna, and M. L. Klein, J. Chem. Phys. **99**, 2796 (1993).
[43] G. Mazzola, S. Yunoki, and S. Sorella, Nature Communications **5**, 3487 (2014).
[44] K. Banerjee and S. P. Bhatnagar, Phys. Rev. D **18**, 4767 (1978).
[45] A. Garg, J. Math. Phys **39**, 5166 (1998).
[46] E. Farhi, J. Goldstone, S. Gutmann, and M. Sipser, quant-ph/0001106.
[47] F. Krzakala, A. Rosso, G. Semerjian, and F. Zamponi, Phys. Rev. B **78**, 134428 (2008).
[48] Z. Jiang, V. N. Smelyanskiy, S. V. Isakov, S. Boixo, G. Mazzola, M. Troyer, and H. Neven, arXiv:1603.01293.
[49] B. Damski and M. M. Rams, Journal of Physics A: Mathematical and Theoretical **47**, 025303 (2014).
[50] M. Okuyama, Y. Yamanaka, H. Nishimori, and M. M. Rams, Phys. Rev. E **92**, 052116 (2015).